Solar water desalination using single-layer solar steam generation systems

Mahmoud Maleki[1], **Farzaneh Arabpour Roghabadi**[1, 2, *], **and Seyed Mojtaba Sadrameli**[3]

[1] *Process Engineering Department, Faculty of Chemical Engineering, Tarbiat Modares University, Tehran, Iran*
[2] *Optoelectronics and Nanophotonics Research Group, Faculty of Electrical and Computer Engineering, Tarbiat Modares University, Tehran, Iran*
[3] *Department of Engineering, German University of Technology in Muscat, Oman*
[*] *Corresponding author email: arabpour@modares.ac.ir*

Manuscript received 28 November, 2021; revised 15 February, 2022; accepted 03 April, 2022. Paper no. JEMT-2111-1352.

Water desalination using solar steam generation systems (SSGSs) is a facile and inexpensive technology that employs a renewable and environmentally friendly source of energy. In this method that solar is directly used for generating steam, a photothermal layer absorbs sunlight and converts it to heat, leading the evaporation of the water transferred toward this layer. Studies show that there are four main challenges in solar steam generation systems that should be considered in research and addressed by providing appropriate solutions. These challenges include managing and preventing heat loss, structural strength, managing and transferring water within the structure, and absorbing and converting light into heat. In this paper, single-layer SSGSs composing of open porosity polyurethane (PU) foam mixed with photothermal materials are used to generate steam. Among the different systems comprising graphite, graphene oxide, carbon nanotube, char, and gold thin film, gold thin film and carbon nanotube based systems resulted the highest performances with an efficiency of more than 60% and the water evaporation rates of 0.824 and 0.808 $Kg.m^{-2}.h^{-1}$, respectively. Fortunately, the device shows no significant changes in its performance after 40 cycles, revealing the suitable stability.

keywords: *Solar water desalination, solar steam generation, single-layer system, photothermal materials, carbon light absorbers.*

http://dx.doi.org/10.22109/jemt.2022.317295.1352

1. INTRODUCTION

Recently, population growth has caused big challenges in providing water for different applications. Fortunately, solar energy as an available, abundant, and free source of energy can be employed to desalinate water via direct and indirect methods. In indirect one, solar electricity is used to provide the energy needed for water desalination. In direct method, solar steam generation systems (SSGSs) are used for production of water steam by absorbing photon energies [1]. Through this process, the sun photons are first collected by the desired light absorbers and then converted into the thermal energy. After that, steam is generated through surface evaporation due to heat localization [2]. These systems should have five important and basic features to increase efficiency and the quality of steam generated including; high light absorption, low thermal conductivity, heat localization, easy water transfer, and finally the ability to float on the water surface [3]. For the first time in 2014, Ghasemi et al. [4] used SSGSs to produce water steam and freshwater. With the help of a two-layer structure based on graphite absorber, they were able to generate steam with 85% efficiency. Since then, many researchers have focused on using different kinds of light absorbers which can be classified into five categories: graphene absorbers, carbon absorbers, wood and plant-based absorbers, nanoparticles absorbers, and polymer absorbers [5]. Among the various structures used for light capturing, the porous structure is a high-potential one which provides more light absorption through scattering, generating more heat and higher temperature and subsequently leads to evaporation of more water. Wilson et al. reported a SSGS based on porous carbon derived from licorice skin (food waste) and polyvinyl alcohol sponge. The system was able to produce steam with an efficiency of 90.88% and a water evaporation rate of 1.386 $Kg.m^{-2}.h^{-1}$ under 1 sun [2]. Huo et al. proposed a porous system based on N-doped graphene/carbon composite aerogels. The introduced system harvested the light efficiently and generated steam with an efficiency of 90 [6]. Carbon aerogel based systems were also considered for this technology. For example, a system with an efficiency of 86.8% was fabricated contained a single-layer of carbon aerogel [7]. Graphene was introduced as an efficient light absorber for SSGSs because of its high absorption coefficient and lightweight. Ito et al. used porous n-doped graphene synthesized by nanoporous Ni based chemical vapor deposition (CVD).

Samples synthesized in different temperatures were compared in terms of WER that they produced. A WER as high as 1.50 $Kg.m^{-2}.h^{-1}$ was achieved for the best sample [8]. On the other hand, as mentioned, heat management plays an essential role in the evaporation process. In fact, the heat generated by the absorption of incident photons can be lost through convective heat transfer and radiation from the upper surface of the system and through the conductive heat transfer from the substrate to the bulk water. In single-layer systems, the use of materials that are both suitable thermal insulator and water transmitters is of particular importance. Compared to the other systems, single-layer systems have two important features, including low construction costs and high structural strength as well as their simplicity. The use of polyurethane (PU) foam as a thermal insulator has been suggested by many researchers [9–11]. In 2017, Shi et al. [12] designed a two-layer SSGS utilizing reduced graphene oxide absorber layer and a polystyrene foam substrate. Using polystyrene foam, the surface temperature of the system showed 10 °C enhancement compared to the system without polystyrene foam. It indicated the ability of polystyrene foam in reducing heat losses to the bulk water and heat localization on the system surface. Finally, they reported that the WER of the introduced system was about 1.31 $Kg.m^{-2}.h^{-1}$ equivalents to 83 efficiency. In another study, PU was used as a suitable substrate for SSGSs. In this system, gold, silver and graphene oxide were deposited on the PU foam as the substrate. The use of these systems led to the production of steam with an efficiency of 60 under 1 sun radiation [13]. Xu et al. fabricated a carbon/sponge evaporator comprising carbonized original leaf particles and commercial melamine sponge. The heat localization and salt-rejection ability were provided by using the upper carbon sponge. It resulted an efficiency of 86.5% under 1 sun [14]. Addition to the aforementioned challenges, systems structural engineering is one of the recent aspects that have been considered by researchers. The device configuration can be significantly effective in increasing the amount of light absorption. Also, through structural engineering, the process of water supply from the water bulk to the surface of the systems can be controlled and managed. Finally, using well engineered structure, the various heat losses can be prevented [15–17]. In the present work, single-layer SSGSs are designed and fabricated. Single-layer SSGSs, known as systems all in one, are generally fabricated with lower costs and have higher mechanical strength compared to other systems due to their integrity. Since self- floating on water is one of the important features in these systems, an open porosity PU foam is used which in addition to self-floating, transfers water to the surface and reduce heat losses, simultaneously. The PU foam has a low conductive heat transfer coefficient. Because PU foam is highly hydrophobic in nature, therefore titanium dioxide (TiO2) nanoparticles are used as a hydrophilic material to improve the water transfer process in single-layer systems. To harvest sun light, various absorbers such as graphite (Gr), graphene oxide (GO), carbon nanotube (CNT), char, and gold thin film are added to the PU curing agent to fabricate single-layer systems. It should be noted that the selected absorbers all are in the category of photothermal materials with high light absorption ability. Some criteria have been considered to select the appropriate photothermal materials comprising the light absorption coefficient, the morphological structure, the cost and availability, and the processability. Carbon-based materials such as graphite, activated carbon, graphene, and carbonized plant and woods, and graphene oxide are widely used as the promising photothermal materials. The main characteristic of this category of material is its high absorption ability (up to 97) that introduced them as promising absorbers in solar thermal applications [5]. Furthermore, they are fabricated through various methods, providing its availability. In order to study the structure of the systems, images taken by optical microscopy, UV-Vis spectroscopy, and contact angle of the layers are considered. To study the performance of the systems, the mass and temperature changes of the water during operation are recorded and used to measure the WER and efficiency.

2. METHODS & MATERIALS

A. materials

An open porosity PU foam is used as a water transfer layer and thermal insulator. To fabricate SSGSs, the desired light absorber is firstly added to foam curing agent (ISO8001) in a certain amount and poured into the mold. PU resin (HR330, Mokararr Co., Iran) is then added to the curing agent. Also Gr, GO, CNT and TiO_2 are all purchased from Sigma. More details related to the different samples fabricated in this work are summarized in 1. Moreover, 1 depicts the photo of these samples. For Au based sample, a thin layer of gold (40 nm) is deposited on the surface of PU foam mixed with TiO_2 using sputtering technique. Since the thickness of the gold layer is nano-scale and deposition of a uniform layer on the PU foam is not expected because of its porous structure, similarly we consider the gold system as a single layer system.

Table 1. Details of the fabricated systems

Sample Name	Absorber		Density	
		(mg)	Dry (gr.cm-3)	Wet (gr.cm-3)
SINLAY 01	TiO_2	60	0.063	0.275
SINLAY 02	TiO_2	60	0.071	0.329
	Gr	600		
SINLAY 03	TiO_2	60	0.078	0.298
	GO	20		
SINLAY 04	TiO_2	60	0.070	0.284
	CNT	400		
SINLAY 05	TiO_2	60	0.050	0.250
	Char	700		
SINLAY 06	TiO_2	60	0.064	0.280
	Thin film of Au	400 (nm)		

B. method

2 provides a general schematic of the process used to evaluate the performance of the SSGSs. SSGSs are illuminated under a sun simulator (380 to 900 nm) with 100 $mWcm^{-}2$ intensity for 30 minutes (No .1). A water container (No. 2) is used to float the samples on the water surface. The systems and their insulation chamber are placed on a digital scale with an accuracy of 0.01 gr (No. 3). To record the images of the temperature distribution through the systems during operation, an infrared thermal camera (OLIP ThermoCam P200) is used. During the operation, temperature and water mass changes are measured. All evaporation tests are conducted under a sun simulator at steady-state conditions. During the analysis, the ambient temperature is kept in the range of 24-25 °C. Also, the water used in this study is from the Caspian seawater containing 4500 ppm Na^{+}, 500 ppm

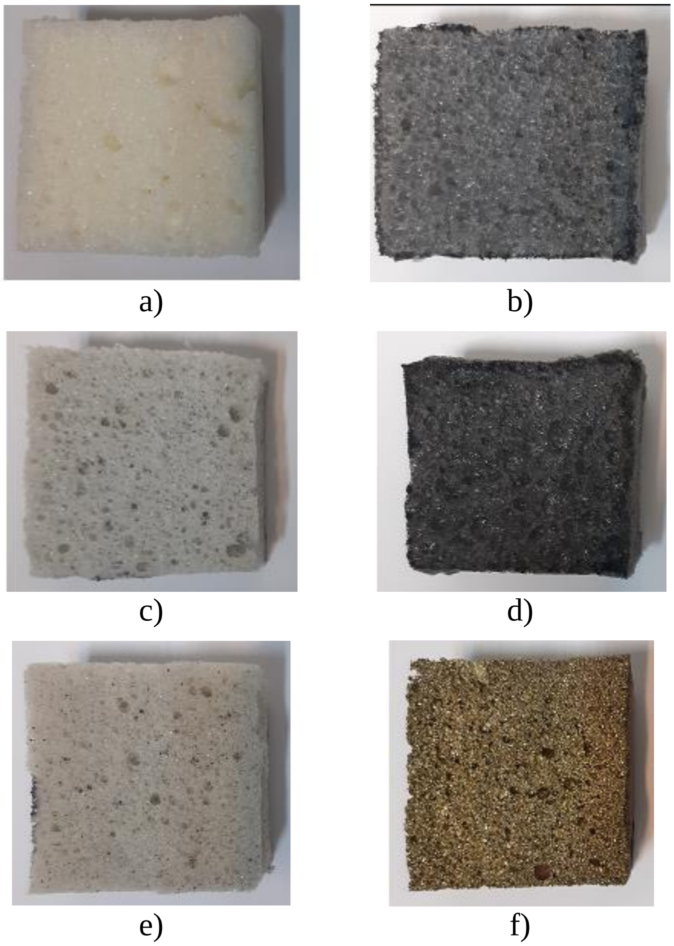

Fig. 1. Photos of the systems fabricated in this work: a) $PU + TiO_2$(without absorber), b) $PU + TiO_2 + Gr$ absorber, c) $PU + TiO_2 + GO$ absorber,d) $PU + TiO_2 + CNT$ absorber, e) $PU + TiO_2$+char absorber, f) $PU + TiO_2$+gold absorber

$Mg^{+}2$, 200 ppm $Ca^{+}2$, and 100 ppm K^{+} ions. In the typical process, when the device floats on the surface of water under sun irradiation, incident photons are absorbed by the photothermal materials and subsequently converted into heat. Simultaneously, water transferred from the bulk to the surface is evaporated and produce steam. Finally, the steam is condensed, providing fresh water.

C. theory

In order to measure the performance of the SSGSs, there are two main parameters that should be evaluated including WER and efficiency. 1 is used to determine the WER:

$$\dot{m} = \frac{W}{A} \quad \textbf{(1)}$$

In the above relation, $\dot{m}$ is the WER, representing the water produced per unit time. Also, W and A are the changes in water mass and the surface area of the SSGS, respectively. (2) is also used to measure the efficiency of the SSGSs:

$$\eta = \frac{\dot{m}h_{fg}}{C_{op}p} \quad \textbf{(2)}$$

In the above relation η is efficiency, $\dot{m}$ is the WER in

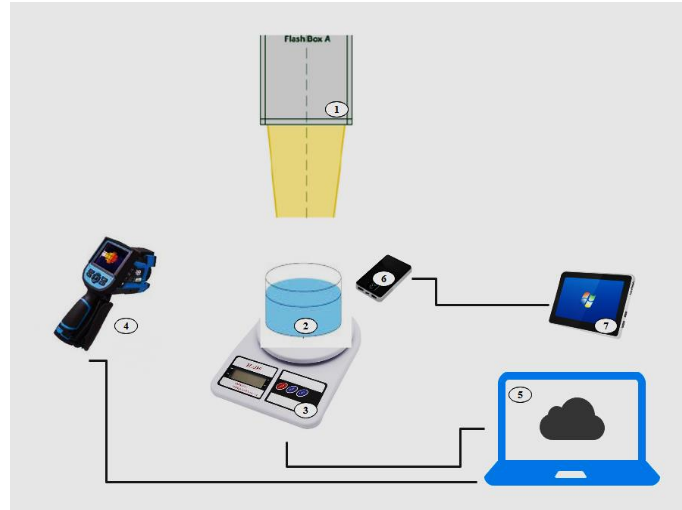

Fig. 2. Schematic of the process: 1) Solar simulator, 2) Water container, 3) Digital scale, 4) Thermal camera, 5) Computer, 6) Power meter, 7) Power meter screen

$Kg.m^{-}2.h^{-}1$. Also, h_{fg} is the enthalpy of phase change is in $Kj.Kg^{-}1$ and C_{op} is the density of sunlight. Further, p is the intensity of light radiation in terms of $KW.m^{-}2$.

3. RESULTS AND DISCUSSION

In 3, images taken by optical microscopy from the surface of all samples are presented. It clearly shows the porous structure of PU and its pore size. The porosity provides more photon absorption through scattering. Further, since the water rising needs to be controlled through the system, the pores cause the well management of this process. As observed, in the presence of photothermal materials, the diameter of the pores is slightly increased. On the other hand, the addition of TiO_2 nanoparticles as a hydrophilic material to the PU foam and on their surface can have a favorable effect on the process of water transfer within systems.

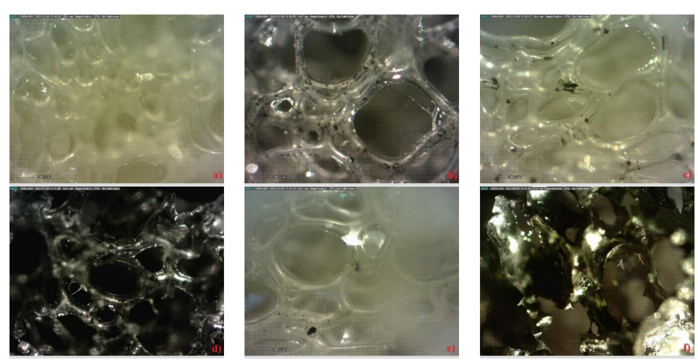

Fig. 3. Optical microscopy images of the system surface: a) $PU + TiO_2$ (without absorbent), b) PU+TiO2+Gr absorbent, c) $PU + TiO_2$+GO absorbent, d) $PU + TiO_2$+CNT absorbent, e) $PU + TiO_2$+char absorbent, f) $PU + TiO_2$+gold absorbent

Since one of the main properties of these systems is the ability of floating on the water surface, the fabricated systems are evaluated to check this ability. So, in these experiments, the fabricated

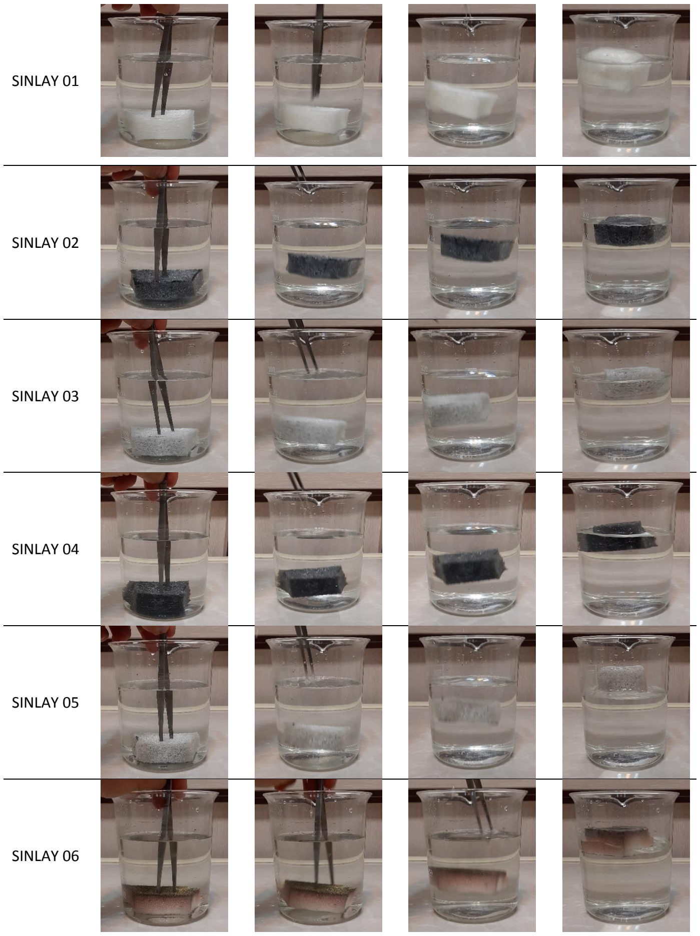

Fig. 4. Self-floating test images for single-layer systems: a) SSGS without absorbent (SINLAY 01), b) SSGS with Gr absorbent (SINLAY 02), c) SSGS with GO absorbent (SINLAY 03), d) SSGS with CNT absorbent (SINLAY 04), e) SSGS with char absorbent (SINLAY 05), f) SSGS with gold absorbent (SINLAY 06)

systems are placed at the bottom of the water container and then released to return to the surface of the water. As shown in 4, among the different structures, all have the ability to self-floating and can float well on the surface of the water. This experiment is one of the recent experiments that have been considered by researchers and can provide a good view of the systems in order to industrialize and float them on the surface of the seas and oceans.

The images related to the contact angle of the surface of the single-layer system without absorber, with Gr absorber, with GO absorber, with CNT absorber, with char absorber, and with gold thin film absorber are presented in 5**a-f** . Since PU foam is highly hydrophobic (contact angle more than 130 degrees), adding TiO_2 makes it hydrophilic and reduces its contact angle to 41.45 degrees. The images also show that with the addition of various absorbers, their hydrophilic properties are slightly reduced, but they are still hydrophilic and do not cause major disruptions in the water transfer process. The single-layer system with Gr absorber shows a contact angle of 117.13 degrees which is more hydrophilic than PU foam with a contact angle of 136 degrees, but more hydrophobic than other systems. Also, single-layer systems with GO absorber and CNT absorber show

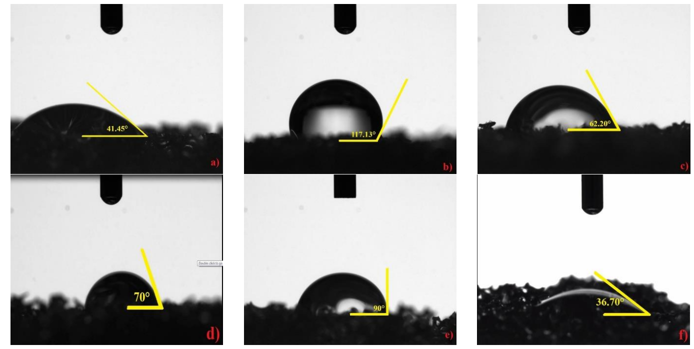

Fig. 5. Surface contact angle images of single-layer systems: a) $PU + TiO_2$(without absorbent), b) $PU + TiO_2$+Gr absorbent, c) $PU + TiO_2$+GO absorbent, d) $PU + TiO_2$+CNT absorbent, e) $PU + TiO_2$+char absorbent, f) $PU + TiO_2$+gold absorbent

contact angles of 62.20 and 70 degrees, respectively. The contact angle of the single-layer system with the char absorber is also measured to be 90 degrees. Finally, the single-layer system with a thin layer of the gold absorber, which is a highly hydrophilic system, has a contact angle of 36.70 degrees. The images related to the thermography camera of the surface of the different single-layer systems are depicted in 6. The initial temperature of all systems is controlled to be 24±0.5°C. After 30 min light irradiation, the surface temperature of the systems is measured again. The temperature profiles indicate the ability of all systems to localize heat on the surface and a significant increase in surface temperature, leading the enhancement of water evaporation rate. Also, the comparison of temperature profiles of different systems shows that, due to the temperature difference between the water bulk and the sample surface, all systems are able to reduce heat loss to the water bulk, which is one of the most important losses in these systems. According to 6, the difference between the surface temperature of the SINLAY 04 sample before and after the test and the difference between its surface temperature and the water bulk are 20.8°C and 18.1°C, respectively. As observed in 6**d**, in contrast to the other samples, the temperature of the surface of the gold sample is low. The reason for observing this can be addressed to the location of the gold which is just on the surface and more hydrophilic nature of the system. It reveals that the heat generated in the system rapidly is consumed for steam generation, causing the low temperature on the surface. To study the performance of the SSGSs, the amount of water mass change is measured and used for calculation of WER and efficiency of systems. As shown in 7, the mass change of the CNT sample (SINLAY 04) is 1.01 gr and char sample (SINLAY 05) is 0.9 gr, whereas this value for the Gr sample (SINLAY 02), GO sample (SINLAY 03) sample, and single-layer system without absorber (SINLAY 01) is 0.975 gr, 0.855 gr, and 0.76 gr, respectively. Also, a water mass change of 0.5 gr is achieved for pure water sample (7). Surprisingly, the amount of water mass changes by single-layer system with gold thin layer absorber (SINLAY 06) reaches 1.03 gr, which is more than 2 times of this value for uncovered water. As can be seen in 8, a study of the performance of single-layer SSGSs shows that the water evaporation rate in these types of systems is on average 1.5 to 2 times that of uncovered water. SINLAY 06 and SINLAY 04 single-layer systems, which are based on gold thin film and CNT absorbers, have the highest water evaporation rates among single-layer systems which are 0.824 $Kg.m^{-2}.h^{-1}$

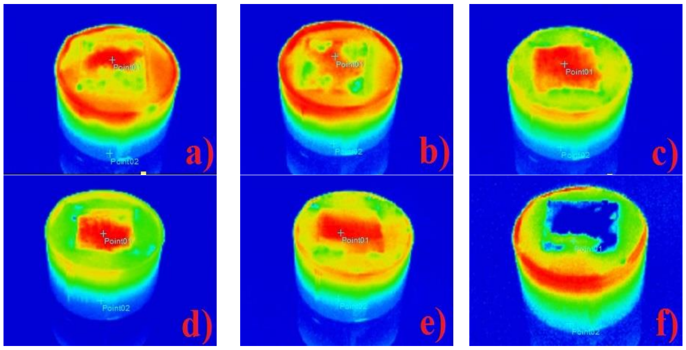

Fig. 6. Surface thermography images of single-layer systems: a) SSGS without absorbent (SINLAY 01), b) SSGS with Gr absorbent (SINLAY 02), c) SSGS with GO absorbent (SINLAY 03), d) SSGS with CNT absorbent (SINLAY 04), e) SSGS with char absorbent (SINLAY 05), f) SSGS with gold absorbent (SINLAY 06)

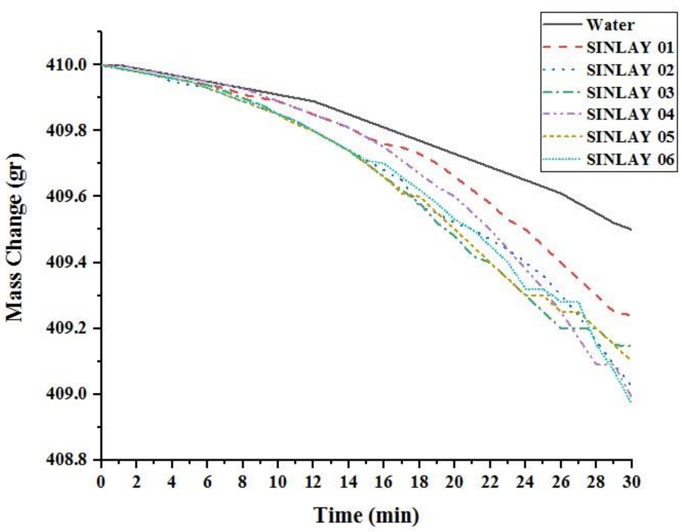

Fig. 7. Graph of water mass changes in single-layer systems; Water: uncovered water, SINLAY 01: SSGS without absorbent, SINLAY 02: SSGS with Gr absorbent, SINLAY 03: SSGS with GO absorbent, SINLAY 04: SSGS with CNT absorbent, SINLAY 05: SSGS with char absorbent, SINLAY 06: SSGS with gold absorbent

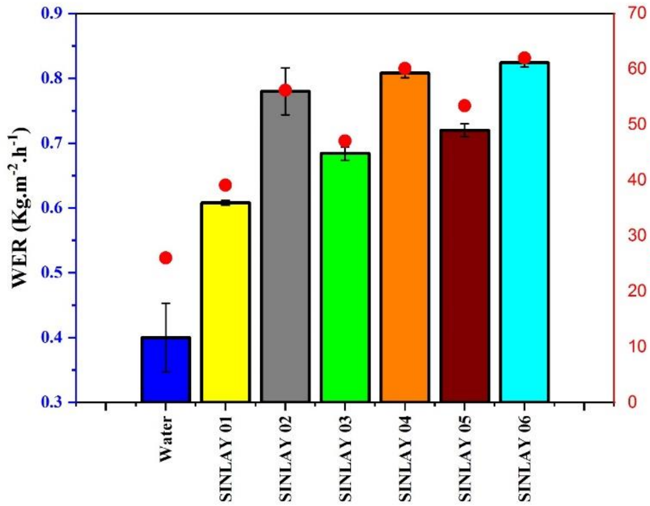

Fig. 8. Graph of water evaporation rate and efficiency of single-layer solar steam generation systems; Water: uncovered water, SINLAY 01: SSGS without absorbent, SINLAY 02: SSGS with Gr absorbent, SINLAY 03: SSGS with GO absorbent, SINLAY 04: SSGS with CNT absorbent, SINLAY 05: SSGS with char absorbent, SINLAY 06: SSGS with gold absorbent

and 0.808 $Kg.m^{-2}.h^{-1}$, respectively. It should be noted that on average, single-layer SSGSs are able to provide an efficiency up to 60%. The gold absorber has plasmonic effects in the range of the sun wavelength, which causes more heat to be generated on the surface of the samples [18]. Addition to the plasmonic absorption of gold system, it seems that its more hydrophilic feature provides well transferring of water, leading the generation of more steam. Moreover, since the gold absorber is just located on the top of the substrate, the generated heat can be localized more. It means that the conduction heat loss from the bottom side is prevented. In general, the amount of photons absorbed by the system, the ability of the system in preventing the generated heat to be lost, and the amount of the water transferred by the systems are effective factors, resulting these performances for different systems.

Salt deposition in the system is one of the main challenges that SSGSs face. In order to check the stability of the system and the ability to prevent salt deposition in the systems, their performance is evaluated for 40 cycles. The water evaporation rate of SINLAY 06 sample through 40 cycles is depicted in 9. The results show that the changes in the water evaporation rate of the system after 40 repetitions are insignificant, confirming the good stability for the fabricated systems.

4. CONCLUSIONS

In summary, different SSGSs were fabricated using Gr, GO, CNT, char, and gold photothermal materials. The performance of the fabricated devices including the aforementioned photothermal materials were investigated. The use of open porosity PU foam as the substrate in SSGSs reduced heat loss to the water bulk and improved the performance of systems by managing water transfer to the system surface. Moreover, the mechanical strength needed for the system was provided by PU foam. Remarkably, in the presence of PU foam without any absorbers, the water evaporation rate increased 50% compared to the un-

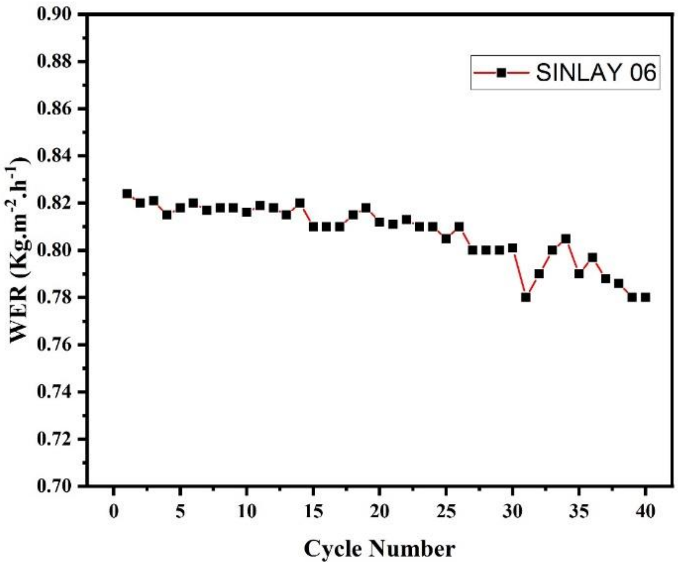

Fig. 9. Water evaporation rate diagram of single-layer SSGSs (for SINLAY 06: SSGS with gold absorbent) through 40 cycles under operation

Table 2. Abbreviations:

Abb.	Description	Abb.	Description
SINLAY 01	Solar steam generation without absorber	SSGS	Solar Steam Generation System
SINLAY 02	Solar steam generation with graphite absorber	PU	Polyurethane
SINLAY 03	Solar steam generation with graphene oxide absorber	TiO2	Titanium Oxide
SINLAY 04	Solar steam generation with carbon nanotube absorber	Gr	Graphite
SINLAY 05	Solar steam generation with char absorber	GO	Graphene Oxide
SINLAY 06	Solar steam generation with gold absorber	CNT	Carbone Nano Tube
WER	Water Evaporation Rate		

covered water (from 0.4 $Kg.m^{-2}.h^{-1}$ to 0.608 $Kg.m^{-2}.h^{-1}$).The water evaporation rates for single-layer systems comprising gold absorber and CNT absorber were 0.824 $Kg.m^{-2}.h^{-1}$ and 0.808 $Kg.m^{-2}.h^{-1}$, respectively, which were 2.06 and 2.02 times that of uncovered water. Furthermore, water evaporation rates of 0.72 $Kg.m^{-2}.h^{-1}$, 0684 $Kg.m^{-2}.h^{-1}$, and 0.78 $Kg.m^{-2}.h^{-1}$ were achieved for the systems containing char, GO, and Gr as the light absorbers, respectively. Among the various absorbers, the gold absorber showed the best performance where its plasmonic effect caused efficient heat generation through light absorption. The achieved performance for gold system can be attributed to the more hydrophilic nature, its plasmonic effect, and less heat losses from the substrate side. Finally, it was proved that the systems are stable and face no significant salt deposition after operation for 40 cycles.

ACKNOWLEDGEMENT

The authors would like to acknowledge the financial support from the research department of Tarbiat Modares University (Research group of phase change materials, Grant No. IG-39710).

REFERENCES

1. Liu, C., Huang, J., Hsiung, C., Tian, Y., Wang, J., Han, Y., Frataloc-chi, A.: High-Performance Large-Scale Solar Steam Generation with Nanolayers of Reusable Biomimetic Nanoparticles. Adv. Sustain. Syst. 1, 1600013 (2017). https://doi.org/10.1002/adsu.201600013
2. Wilson, H.M., Ahirrao, D.J., Raheman Ar, S., Jha, N.: Biomass-derived porous carbon for excellent low intensity solar steam generation and seawater desalination. Sol. Energy Mater. Sol. Cells. 215, 110604 (2020). https://doi.org/10.1016/j.solmat.2020.110604
3. Ni, G., Li, G., Boriskina, S. V., Li, H., Yang, W., Zhang, T., Chen, G.: Steam generation under one sun enabled by a floating structure with thermal concentration. Nat. Energy. 1, 16126 (2016). https://doi.org/10.1038/nenergy.2016.126
4. Ghasemi, H., Ni, G., Marconnet, A.M., Loomis, J., Yerci, S., Miljkovic, N., Chen, G.: Solar steam generation by heat localization. Nat. Commun. 5, 4449 (2014). https://doi.org/10.1038/ncomms5449
5. Karami, S., Arabpour Roghabadi, F., Maleki, M., Ahmadi, V., Sadrameli, S.M.: Materials and structures engineering of sun-light absorbers for efficient direct solar steam generation. Sol. Energy. 225, 747–772 (2021). https://doi.org/10.1016/j.solener.2021.07.046
6. Huo, B., Jiang, D., Cao, X., Liang, H., Liu, Z., Li, C., Liu, J.: N-doped graphene /carbon hybrid aerogels for efficient solar steam generation. Carbon N. Y. 142, 13–19 (2019). https://doi.org/10.1016/j.carbon.2018.10.008
7. Mu, P., Zhang, Z., Bai, W., He, J., Sun, H., Zhu, Z., Liang, W., Li, A.: Superwetting Monolithic Hollow-Carbon-Nanotubes Aerogels with Hierarchically Nanoporous Structure for Efficient Solar Steam Generation. Adv. Energy Mater. 9, 1–9 (2019). https://doi.org/10.1002/aenm.201802158
8. Ito, Y., Tanabe, Y., Han, J., Fujita, T., Tanigaki, K., Chen, M.: Multifunctional Porous Graphene for High-Efficiency Steam Generation by Heat Localization. Adv. Mater. 27, 4302–4307 (2015). https://doi.org/10.1002/adma.201501832
9. Sui, Y., Hao, D., Guo, Y., Cai, Z., Xu, B.: A flowerlike sponge coated with carbon black nanoparticles for enhanced solar vapor generation. J. Mater. Sci. 55, 298–308 (2020). https://doi.org/10.1007/s10853-019-03977-9
10. Li, D., Li, A., Chen, Y., Chen, G., Chen, X., Zhang, D., Zhu, H., Samo, I.A., Song, H.: Spray-freezing induced multidimensional morphology tuning of assembled spherical carbon for solar-driven steam generation. Carbon N. Y. 162, 481–489 (2020). https://doi.org/10.1016/j.carbon.2020.02.085
11. Cai, W., Mu, X., Pan, Y., Li, Z., Wang, J., Zhou, X., Guo, W., Hu, W., Song, L., Hu, Y.: Black Phosphorous Nanosheets: A Novel Solar Vapor Generator. Sol. RRL. 4, 1900537 (2020). https://doi.org/10.1002/solr.201900537
12. Shi, L., Wang, Y., Zhang, L., Wang, P.: Rational design of a bi-layered reduced graphene oxide film on polystyrene foam for solar-driven interfacial water evaporation. J. Mater. Chem. A. 5, 16212–16219 (2017). https://doi.org/10.1039/c6ta09810j
13. Awad, F.S., Kiriarachchi, H.D., Abouzeid, K.M., Özgür, Ü., El-Shall, M.S.: Plasmonic Graphene Polyurethane Nanocomposites for Efficient Solar Water Desalination. ACS Appl. Energy Mater. 1, 976–985 (2018). https://doi.org/10.1021/acsaem.8b00109
14. Xu, K., Wang, C., Li, Z., Yan, X., Mu, X., Ma, M., Zhang, P.: Architecting a Janus biomass carbon/sponge evaporator with salt-rejection and ease of floatation for sustainable solar-driven desalination. Environ. Sci. Water Res. Technol. 7, 879–885 (2021). https://doi.org/10.1039/D1EW00070E
15. Miao, E.-D., Ye, M.-Q., Guo, C.-L., Liang, L., Liu, Q., Rao, Z.-H.: Enhanced solar steam generation using carbon nanotube membrane distillation device with heat localization. Appl. Therm. Eng. 149, 1255–1264 (2019). https://doi.org/10.1016/j.applthermaleng.2018.12.123
16. Zou, Y., Chen, X., Guo, W., Liu, X., Li, Y.: Flexible and Robust Polyaniline Composites for Highly Efficient and Durable Solar Desalination. ACS Appl. Energy Mater. 3, 2634–2642 (2020). https://doi.org/10.1021/acsaem.9b02341
17. Peng, G., Deng, S., Sharshir, S.W., Ma, D., Kabeel, A.E., Yang, N.: High efficient solar evaporation by airing multifunctional textile. Int. J. Heat Mass Transf. 147, 118866 (2020). https://doi.org/10.1016/j.ijheatmasstransfer.2019.118866
18. Liu, X., Wang, X., Zhu, J., He, Y., Cheng, G.: Solar steam generation through bio-inspired interface heating of broadband-absorbing plasmonic membranes. Appl. Energy. 195, 414–425 (2017). https://doi.org/10.1016/j.apenergy.2017.03.080